International Journal of Thermal Sciences 49 (2010) 1133–1137

Contents lists available at ScienceDirect

International Journal of Thermal Sciences

journal homepage: www.elsevier.com/locate/ijts

# Nonlocal behavior in thermal lagging

D.Y. Tzou [a,*], Zeng-Yuan Guo [b]

[a] Department of Mechanical and Aerospace Engineering, University of Missouri, Columbia, MO 65203, USA
[b] Department of Engineering Mechanics, Tsinghua University, Beijing 100084, China

ARTICLE INFO

*Article history:*
Received 5 November 2009
Received in revised form
25 January 2010
Accepted 27 January 2010
Available online 25 February 2010

*Keywords:*
Nonlocal
Lagging
Thermomass
Phonon
Wave

ABSTRACT

Nonlocal behavior during thermal lagging is studied in this work to accommodate the effect of the thermomass (TM) of the dielectric lattices. Perfect correlations are established, with the lagging time in the TM model equivalent to the phase lag of the heat flux vector and the length parameter in the TM model equivalent to the correlating length describing the nonlocal response. Simultaneous existence of the nonlocal (in space) and lagging (in time) behaviors give rise to a new type of thermal waves, which can be many times faster than the Cattaneo–Vernotte waves. Nonlinear behaviors of the phase lag and the correlating length are considered in the general model to study their influences on suppressing the sharp wavefronts. Dominating parameters are extracted to characterize the nonlocal response with thermal lagging.



## 1. Introduction

Ultrafast heat transport that occurs in times comparable to the mean free times of energy carriers is inspired by the advancement of ultrashort pulsed lasers over the past decade [1–7]. Due to the limited number of collisions in such short times, which are of the order of 10 femtoseconds (fs) for electron-to-electron collisions, 1 picosecond (ps) for electron-to-phonon collision, and 10 ps for phonon-to-phonon collisions [8,9], individual behaviors of energy carriers will become pronounced. Consequently, traditional concepts in heat transport based on the averaged behaviors over numerous collisions do not apply. Though phenomenological by nature, the constitutive equation provides a convenient approach in describing the ultrafast physical response. Evolving from Fourier's law describing the quasi-stationary and reversible transition of thermodynamic states, the constitutive equation can be as complicated as the dual-phase-lag (DPL) model [10],

$$\vec{q}(\vec{r},t+\tau_q) = -k\nabla T(\vec{r},t+\tau_T) \Rightarrow \vec{q}(\vec{r},t) + \tau_q \frac{\partial \vec{q}(\vec{r},t)}{\partial t} + \frac{\tau_q^2}{2}\frac{\partial^2 \vec{q}(\vec{r},t)}{\partial t^2} \cong -k\nabla T(\vec{r},t) - k\tau_T \frac{\partial \nabla T(\vec{r},t)}{\partial t} - \frac{k\tau_T^2}{2}\frac{\partial^2 \nabla T(\vec{r},t)}{\partial t^2}, \quad (1)$$

where two phase lags ($\tau_T$ and $\tau_q$) are present due to the delayed response during the ultrafast transient. As shown by the second expression in Eq. (1), the lagging response significantly deviates from Fourier's law due to involvement of the high-order derivatives with respect to time. In the special case of $\tau_T = 0$, the linear effect of $\tau_q$ (i.e., neglecting the $\tau_q^2$ term on the left-hand side of Eq. (1)) reduces to the thermal wave model proposed by Cattaneo [11] and Vernotte [12]. In correlation to the existing microscopic models, in addition, the lagging behavior described by Eq. (1) absorbs electron–phonon coupling in metals [8,9], umklapp (temporary momentum loss) and normal relaxations in phonon scattering [13], and additional relaxation of internal energy [14] in the same framework of thermal lagging. In the absence of volumetric heating, the energy equation accommodating the lagging behavior described by Eq. (1) is [10,15,16],

$$\nabla^2 T + \tau_T \frac{\partial}{\partial t}(\nabla^2 T) + \frac{\tau_T^2}{2}\frac{\partial^2}{\partial t^2}(\nabla^2 T) = \frac{1}{\alpha}\frac{\partial T}{\partial t} + \frac{\tau_q}{\alpha}\frac{\partial^2 T}{\partial t^2} + \frac{\tau_q^2}{2\alpha}\frac{\partial^3 T}{\partial t^3}, \quad (2)$$

which completely alters the fundamental characteristics of Fourier diffusion due to the presence of the mixed-derivative terms and the high-order derivatives of temperature with respect to time.

The high-order terms of $\tau_T$ and $\tau_q$ in Eqs (1) and (2) and result from the gradual expansions of the Taylor series in correlation to other microscopic models. After the linear version involving the linear effects of $\tau_T$ and $\tau_q$, for example, the $\tau_q^2$ term was instated to describe the *T*-waves that can be one order of magnitude faster than the CV-wave. Effects of $\tau_T^2$ were instated recently in describing

* Corresponding author. Tel.: +1 5738824060; fax: +1 5738845090.
*E-mail address:* tzour@missouri.edu (D.Y. Tzou).

1290-0729/$ – see front matter © 2010 Elsevier Masson SAS. All rights reserved.
doi:10.1016/j.ijthermalsci.2010.01.022

**Nomenclature**

| | |
|---|---|
| $C$ | volumetric heat capacity, J m$^{-3}$ K$^{-1}$ |
| $c$ | speed of light, m s$^{-1}$ |
| $c_p$ | specific heat, J kg$^{-1}$ K$^{-1}$ |
| $E$ | total thermal vibration energy of the lattice at rest, J |
| $f$ | resistance force, N m$^{-3}$ |
| $K$ | equivalent conductivity, W m$^{-1}$ K$^{-1}$ |
| $k$ | conductivity, W m$^{-1}$ K$^{-1}$ |
| $L$ | ratio of $\lambda_q$ to $\sqrt{(\alpha\tau_q)}$ |
| $l$ | length parameter in the thermomass model, m |
| $M$ | thermal Mach number |
| $m$ | mass, kg |
| $p$ | pressure, Pa |
| $q$ | heat flux, W m$^{-2}$ |
| $T$ | temperature, K |
| $u$ | drift velocity, m s$^{-1}$ |
| $Z$ | ratio of $\tau_T$ to $\tau_q$ |

*Greek*

| | |
|---|---|
| $\alpha$ | thermal diffusivity, $K/C$, m$^2$ s$^{-1}$ |
| $\beta$ | coefficient of resistance, kg m$^{-3}$ s$^{-1}$ |
| $\lambda_q$ | correlating length, m |
| $\rho$ | density, kg m$^{-3}$ |
| $\tau_q$ | phase lag of the heat flux, s |
| $\tau_T$ | phase lag of the temperature gradient, s |
| $\nabla^2$ | Laplacian |

*Subscripts*

| | |
|---|---|
| CV | Cattaneo–Vernotte |
| $h$ | phonon gas |
| NL | nonlocal with lagging |
| R | at rest |
| TM | thermomass |

*Superscripts*

| | |
|---|---|
| $\vec{X}$ | vector of $X$ |

transport phenomena in biological systems with multiple energy carriers [15,16].

Describing the phonon gas in the dielectrics as a weighty and compressible fluid, the thermomass (TM) model [17,18] distinguishes itself from others by accommodating the equivalent mass of the phonon gas calculated from the Einstein's mass–energy relation. The distinctive mass of heat thus defined, termed thermomass, makes the TM model unique in *deriving* the energy and constitutive equations from the continuity and Newton's law (momentum equations) for the weighty and compressible phonon flow. In view of the TM model, most remarkably, thermal and mechanical fields are mutually implied, which provides a resolution addressing Fourier's statement made in 1822, that "…But whatever may be the range of mechanical theories, they do not apply to the effects of heat. These make up a special order of phenomena, which cannot be explained by the principles of motion and equilibrium…".

This work incorporates the nonlocal behavior in thermal lagging to capture the effect of the thermomass of phonon gas in dielectrics. Coexisting with the phase lag of the heat flux vector, $\tau_q$ in Eq. (1), it will be shown that instating a correlating length in space is equivalent to the TM model. The nonlocal behavior with thermal lagging results in a new type of wave that propagates faster than the CV-wave. The sharp wavefront carrying an infinite time-rate of change of temperature (in time, or temperature gradient in space), however, inherits the same deficiency as that in the classical CV-wave. Effect of $\tau_T$ thus follows to illustrate dispersion of the sharp wavefront due to the phase lag of the temperature gradient. Since nonlocal behavior in thermal lagging is pertinent to the ultrafast transient, an important task of the present study is to identify the dominating parameters that could be used in the experimental studies. Nondimensional analysis will be introduced for this purpose to characterize the nonlocal response with thermal lagging.

## 2. Thermomass model

Key quantities in the TM model [17,18] are the thermomass density of the phonon gas ($\rho_h$), the drift velocity ($u_h$), the pressure ($p_h$) of the phonon gas induced by the thermal vibration of the lattice, and the resistance force per unit volume ($f_h$):

$$\rho_h = \frac{CT}{c^2}, \quad u_h = \frac{q}{CT}, \quad p_h = \frac{\gamma c^2 \rho_h^2}{\rho}, \text{ and } f_h = \beta u_h. \tag{3}$$

The thermomass density ($\rho_h$) is calculated from the volumetric average of the thermomass ($m_h$) of the lattice, $m_h = E/c^2$ resulting from the Einstein's mass–energy relation with $E = m_R c_p T$ representing the thermal vibration energy stored in the lattice at rest. Heat flux ($q$) is carried with the drift velocity ($u_h$) of the phonon gas in which the volumetric energy density is $CT$. The phonon gas pressure ($p$) is derived from the Debye's equation of state involving the Grüneisen constant ($\gamma$). By substituting the first expression in Eq. (3) for $\rho_h$, it can be readily seen that the phonon gas pressure is proportional to its temperature squared, which is exactly the same behavior as that in the electron gas in metals [7]. The resistance force results from the gradient of the phonon gas pressure, $f_h = -dp_h/dx$, and the Darcy's law that describes phonon scattering through the porous dielectrics. The resistance coefficient ($\beta$) is the proportional constant between $f_h$ and $u_h$. In its most generic form, $\beta = 2\gamma C^3 T^2/(\rho k c^2)$.

Resulting from the concept of mass of heat, the mechanical and thermal fields become mutually implied in the TM model. In the case of one-dimensional heat conduction, from Eq. (3), the continuity equation reduces to the energy equation in the phonon gas,

$$\frac{\partial \rho_h}{\partial t} + \frac{\partial}{\partial x}(\rho_h u_h) = 0 \Rightarrow -\frac{\partial q}{\partial x} = C\frac{\partial T}{\partial t}. \tag{4}$$

The momentum equation, on the other hand, reduces to the constitutive equation for the phonon gas,

$$\rho_h \overbrace{\left(\frac{\partial u_h}{\partial t} + u_h \frac{\partial u_h}{\partial x}\right)}^{\frac{Du_h}{Dt}} + \frac{\partial p_h}{\partial x} + f_h = 0 \Rightarrow \tau_{TM}\frac{\partial q}{\partial t} - lC\frac{\partial T}{\partial t} + l\frac{\partial q}{\partial x} - M^2 k\frac{\partial T}{\partial x} + k\frac{\partial T}{\partial x} + q = 0, \tag{5}$$

where $\tau_{TM}$ is the lagging time in the thermomass model, which is about two orders of magnitude larger than the relaxation time of phonons in the CV-wave model, $l = qk\rho/[2\gamma C(CT)^2]$ is a length parameter, and $M$ is the thermal Mach number of the drift velocity relative to the thermal wave speed in the phonon gas. In the second expression in Eq. (5), the first four terms on the left-hand side results from the inertia effect, $\rho_h(Du_h/Dt)$. The fifth term results from the pressure gradient of the phonon gas, and the last term results from the resistance force since $f_h = \beta u_h = \beta q/(CT)$ from Eq. (3).

Eliminating heat flux ($q$) from Eqs. (4) and (5), it results in an energy equation containing temperature ($T$) alone:

$$\frac{k(1-M^2)}{C\tau_{TM}}\frac{\partial^2 T}{\partial x^2} = \frac{1}{\tau_{TM}}\frac{\partial T}{\partial t} + \frac{2l}{\tau_{TM}}\frac{\partial^2 T}{\partial x \partial t} + \frac{\partial^2 T}{\partial t^2}. \quad (6)$$

In addition to the wave behavior described by the second order derivative with respect to time, $\partial T^2/\partial t^2$, Eq. (6) contains a mixed-derivative term, $\partial T^2/\partial x\partial t$, which is something new to the field of microscale heat transfer. The DPL model does involve similar mixed-derivative terms, but they are of the even orders with respect to $x$ [10]. Note that the length parameter ($l$) in Eq. (6) is proportional to the heat flux ($q$). As the space coordinate ($x$) is reversed to the negative direction, the heat flux switches its sign accordingly, which satisfies the symmetric principle for any physically admissible constitutive relations [10].

## 3. Nonlocal behavior

Involvement of a length parameter in Eq. (6) is enlightening to include the nonlocal behavior, in space, in addition to the lagging response in time:

$$q(x+\lambda_q, t+\tau_q) = -K\frac{\partial T}{\partial x}(x,t). \quad (7)$$

Equivalence between the nonlocal behavior in space and the lagging response in time has been established [10], but a simultaneous consideration for both has not been made yet due to the lack of a constitutive model supporting such an expansion. Aiming at the correlation to the TM model, the phase lag of the heat flux ($\tau_q$) is assumed small in comparison with the process time ($t$), and the correlating length ($\lambda_q$) is assumed small in comparison with the space dimension ($x$). The Taylor series expansion of Eq. (7) containing the first-order effects of $\tau_q$ and $\lambda_q$ then yields

$$q(x,t) + \lambda_q\frac{\partial q(x,t)}{\partial x} + \tau_q\frac{\partial q(x,t)}{\partial t} \cong -K\frac{\partial T}{\partial x}(x,t). \quad (8)$$

Eliminating heat flux ($q$) from Eq. (8) and the conventional energy equation,

$$-\frac{\partial q}{\partial x} = C\frac{\partial T}{\partial t}, \quad (9)$$

The result is

$$\left(\frac{K}{C\tau_q}\right)\frac{\partial^2 T}{\partial x^2} = \frac{1}{\tau_q}\frac{\partial T}{\partial t} + \left(\frac{\lambda_q}{\tau_q}\right)\frac{\partial^2 T}{\partial x \partial t} + \frac{\partial^2 T}{\partial t^2}. \quad (10)$$

Equation (10) obtained from the nonlocal response with thermal lagging (the NL model) has exactly the same form as Eq. (6) obtained from the TM model, resulting in

$$K = k(1-M^2), \quad \tau_q = \tau_{TM}, \quad \lambda_q = 2l. \quad (11)$$

While the phase lag of the heat flux ($\tau_q$) is equivalent to the lagging time ($\tau_{TM}$) in the thermomass model, the correlating length ($\lambda_q$) in the NL model simply stretches the length parameter ($l$) in the TM model by two times. With the perfect correlation thus established, clearly, the NL model is equivalent to the TM model in capturing the effect of heat mass for heat transport in dielectrics.

### 3.1. Effect of $\tau_T$

Equation (10) represents a new type of energy equation in microscale heat transport, even though it is mathematically simpler than the DPL heat equation that contains a third-order, mixed-derivative term. Since the derivative of the highest order remains to be with the wave term, $\partial^2 T/\partial t^2$, a sharp wavefront will continue to exist like the CV-wave. The NL-wave, as shown below, will be faster than the CV-wave but both will suffer from the same singularities in the time-rate of change of temperature ($\partial T/\partial t$) and temperature gradient ($\partial T/\partial x$) across the wavefront. To remove such singularities, in parallel to the previous treatment of the CV-wave, the phase lag of the temperature gradient ($\tau_T$) is further introduced in Eq. (7),

$$q(x+\lambda_q, t+\tau_q) = -K\frac{\partial T}{\partial x}(x, t+\tau_T). \quad (12)$$

The first-order expansion in $\tau_T$, $\tau_q$, and $\lambda_q$ reads

$$q(x,t) + \lambda_q\frac{\partial q(x,t)}{\partial x} + \tau_q\frac{\partial q(x,t)}{\partial t} = -K\frac{\partial T}{\partial x}(x,t) - K\tau_T\frac{\partial^2 T}{\partial x \partial t}(x,t), \quad (13)$$

and the energy equation in correspondence with Eq. (10) becomes

$$\left(\frac{K}{C\tau_q}\right)\frac{\partial^2 T}{\partial x^2} + \left(\frac{K\tau_T}{C\tau_q}\right)\frac{\partial^3 T}{\partial x^2 \partial t} = \frac{1}{\tau_q}\frac{\partial T}{\partial t} + \left(\frac{\lambda_q}{\tau_q}\right)\frac{\partial^2 T}{\partial x \partial t} + \frac{\partial^2 T}{\partial t^2}. \quad (14)$$

There are two mixed-derivative terms in Eq. (14), which recovers Eq. (10) as $\tau_T \to 0$. The derivative of the highest order now shifts to the third-order mixed-derivative term, $\partial^3 T/\partial x^2 \partial t$, which efficiently removes the singularities across the wavefront even with a small value of $\tau_T$ [10]. For heat transport in dielectrics, $\tau_q$ is the same as the umklapp relation time while $\tau_T$ results from a simple stretch from the normal relaxation time by (9/5) times.

All expressions have been derived for the one-dimensional response. The general forms of Eqs. (9) and (13) are

$$-\nabla\cdot\vec{q} = C\frac{\partial T}{\partial t} \text{ and } \vec{q} + (\vec{\lambda}_q\cdot\nabla)\vec{q} + \tau_q\frac{\partial\vec{q}}{\partial t} = -K\nabla T - K\tau_T\frac{\partial}{\partial t}\nabla T, \quad (15)$$

which yields

$$\left(\frac{K}{C\tau_q}\right)\nabla^2 T + \left(\frac{K\tau_T}{C\tau_q}\right)\frac{\partial}{\partial t}\nabla^2 T - \left(\frac{1}{\tau_q}\right)\vec{\lambda}_q\cdot\nabla\left(\frac{\partial T}{\partial t}\right) = \frac{1}{\tau_q}\frac{\partial T}{\partial t} + \frac{\partial^2 T}{\partial t^2} \quad (16)$$

for describing the nonlocal response with thermal lagging in a three dimensional conductor. The nonlocal term involving $\vec{\lambda}_q$ not only introduces another mixed-derivative in DPL, it also has a sign difference as compared to the thermalization term involving $\tau_T$ on the left-hand side of Eq. (16).

## 4. Results and discussion

New types of energy equations have been resulted from the nonlocal response in the presence of thermal lagging: Equation (10) containing the linear effect of $\lambda_q$ and $\tau_q$ and (14) containing an additional effect of $\tau_T$. Equation (14) will be used to study the fundamental characteristics of the nonlocal behavior with thermal lagging because it covers Eq. (10) as a special case as $\tau_T$ is set to zero.

To illustrate the nonlocal effect in thermal lagging, let us consider a one-dimensional, semi-infinite solid initially kept a constant temperature $T_0$, as sketched in Fig. 1. The solid is disturbed from a stationary state, $\partial T/\partial t = 0$ as $t = 0$. The surface at $x = 0$ is suddenly raised to a constant temperature $T_w$, which drives the thermal disturbance to propagate downstream. At a distance sufficiently far from the heated surface, the temperature recovers its initial value. Introducing

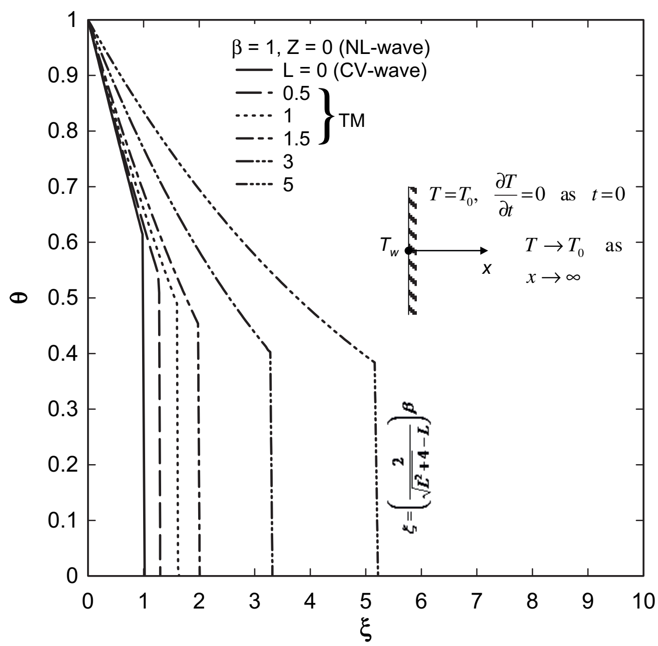


**Fig. 1.** Effect of correlating length ($L$) on the nonlocal behavior in thermal lagging: The case of $L = 0$ reduces to the CV-wave model and the cases of $L < 2$ are in correlation to the TM model.

$$\xi = \frac{x}{\sqrt{\alpha\tau_q}}, \quad \beta = \frac{t}{\tau_q}, \quad \theta = \frac{T - T_0}{T_W - T_0}, \quad Z = \frac{\tau_T}{\tau_q}, \quad \text{and } L = \frac{\lambda_q}{\sqrt{\alpha\tau_q}}, \tag{17}$$

Eq. (14) and the initial/boundary conditions become

$$\frac{\partial^2\theta}{\partial\xi^2} + Z\frac{\partial^3\theta}{\partial\xi^2\partial\beta} = \frac{\partial\theta}{\partial\beta} + L\frac{\partial^2\theta}{\partial\xi\partial\beta} + \frac{\partial^2\theta}{\partial\beta^2} \tag{18}$$

$$\theta(\xi,0) = \frac{\partial\theta}{\partial\beta}(\xi,0) = 0; \quad \theta(0,\beta) = 1 \text{ and } \theta(\xi,\beta)\to 0 \text{ as } \xi\to\infty \tag{19}$$

Clearly, the nonlocal response with thermal lagging is characterized by two parameters, $Z$ and $L$ as defined in Eq. (17). The Laplace transform solution to Eqs. (13) and (14) is

$$\overline{\theta}(\xi;p) = \exp\left[\frac{\left(Lp - \sqrt{(Lp)^2 + 4p(p+1)(1+Zp)}\right)\xi}{2}\right]\Big/ p \tag{20}$$

*4.1. Effect of $\lambda_q$ and $\tau_q$*

Equation (20) with $Z = 0$ ($\tau_T = 0$) reduces to the nondimensional solution to Eq. (10) in correlation to the NL/TM model:

$$\overline{\theta}_{NL}(\xi;p) = \exp\left[\frac{\left(Lp - \sqrt{(Lp)^2 + 4p(p+1)}\right)\xi}{2}\right]\Big/ p \tag{21}$$

It can be shown by the partial expansion technique [10] along with the limiting theorem in the Laplace transform that Eq. (21) represents a wave with a sharp wavefront located at

$$\xi = \left(\frac{2}{\sqrt{L^2+4} - L}\right)\beta, \quad \text{or } x = c_{NL}t \text{ with } c_{NL} = \sqrt{c_{CV}^2 + \left(\frac{c_q}{2}\right)^2} + \frac{c_q}{2}$$

where $$c_{CV} = \sqrt{\frac{\alpha}{\tau_q}}, \quad c_q = \frac{\lambda_q}{\tau_q} \tag{22}$$

Clearly, $c_{NL} > c_{CV}$, implying the NL-wave propagating faster than the classical CV-wave. Note that $c_q = 2u_h$ and $L = \lambda_q/\sqrt{(\alpha\tau_q)} = c_q/c_{CV} = 2M$ in correlation with the TM model. Since $u_h << c_{CV}$, the condition of $M < 1$ prevails in the TM model, which implies $L < 2$ in the correlation. Involvement of $\tau_q$, which is equivalent to the mean free time, and $u_h$ (through $c_q$) implies that the correlating length ($\lambda_q$) is of the same order as the mean free path in phonon scattering.

Laplace inversion of Eq. (15) can be furnished by the Riemann sum approximation [10]:

$$\theta(\xi,\beta) \cong \frac{e^{4.72}}{\beta}\left[\frac{1}{2}\overline{\theta}\left(\xi; p = \frac{4.72}{\beta}\right) + \text{Re}\sum_{n=1}^{N}\overline{\theta}\left(\xi; p = \frac{(4.72 + in\pi)}{\beta}\right)(-1)^n\right]. \tag{23}$$

Codes written in both Fortran [10] and Mathematica [19], with the default local and global accuracies set in Mathematica for assuring the numerical convergence, are available to evaluate the infinite series in Eq. (23). For $Z = 0$ ($\tau_T = 0$) and $\beta = 1$ ($t = \tau_q$), resulting from the use of $\overline{\theta}_{NL}$ given by Eq. (21) in place of $\overline{\theta}$ in Eq. (23), Fig. 1 shows the effect of $L$ on the spatial distributions of the NL-wave, for which the wavefront is located at $\xi = 2/[\sqrt{(L^2+4)} - L]$. Since $Z = 0$ ($\tau_T = 0$), the case of $L = 0$ ($\lambda_q = 0$) reduces to the classical CV-wave. The wavefront of the NL-wave advances from $\xi = 1$ ($L = 0$), 1.281 ($L = 0.5$), 1.618 ($L = 1$), 2 ($L = 1.5$), 3.303 ($L = 3$), 5.193 ($L = 5$) as the value of $L$ increases. The temperature level in the heat affected zone behind the thermal wavefront increases with the value of $L$. The cases with $L = 0.5$, 1, and 1.5 ($L < 2$) are in correlation with the TM model since $L = 2M$ and $M < 1$ in the phonon gas. The correlating length ($\lambda_q$) and the phase lag of the heat flux vector ($\tau_q$) appear as two material dependent constants in the NL model, with $\tau_q$ correlating to the mean free time and $\lambda_q$ correlating to the mean free path in microscale heat transfer. The ratio, $L = \lambda_q/\sqrt{(\alpha\tau_q)}$, therefore, could be greater than two in general without establishing a correlation to the TM model. The cases of $L = 3$ and 5 are added in Fig. 1 for the sake of generality which, however, continue the general trend in the cases of $L < 2$.

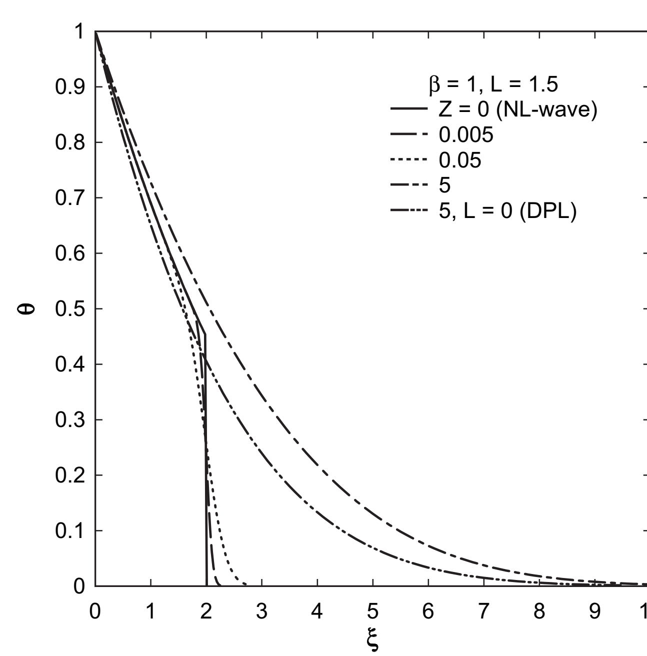


**Fig. 2.** Effect of thermal lagging ($Z$) on the nonlocal response: The case of $Z = 0$ corresponds to the NL/TM wave and the case of $L = 0$ corresponds to the dual-phase-lag model without the nonlocal behavior.

Both the NL- and CV-waves result in a sharp wavefront in transition from the heat affected zone ($\xi < 2\beta/[\sqrt{(L^2+4)} - L]$) to the thermally unaffected zone ($\xi > 2\beta/[\sqrt{(L^2+4)} - L]$). Consequently, as shown in Fig. 1, temperature gradient approaches infinity across the wavefront, which may be seen as a paradox in any wave model as compared to the infinite speed of heat propagation in Fourier diffusion. The phase lag of the temperature gradient, the mixed-derivative term containing $\tau_T$ shown in Eq. (14), is effective in removing such a singularity at the wavefront. In the presence of the nonlocal response, $L = 1.5$, Fig. 2 describes the ways in which a sharp wavefront is well spread by the effect of $\tau_T$. As the value of $Z$ ($=\tau_T/\tau_q$) is slightly disturbed from 0, evidenced by the curve of $Z = 0.005$, a finite but large temperature gradient still exists near $\xi = 2$ but the transition from the heat affected zone ($\xi < 2$) to the thermally unaffected zone ($\xi > 2$) becomes smooth. This is more evident as the value of $Z$ further increases to 0.05, as shown by the dotted curve in Fig. 2. The wavefront is totally destroyed as the value of $Z$ increases to 5 (dot–dash). The temperature level increases with the value of $Z$. As compared to the case of DPL with $L = 0$ (dot–dot–dash), $\tau_T \neq 0$ but $\lambda_q = 0$ at the same value of $Z = 5$, the nonlocal response (dot–dash) results in a higher temperature than DPL (dot–dot–dash).

## 5. Conclusion

Nonlocal response, in space, has been extended in the DPL model to capture the effect of heat mass described in the TM model. In the absence of the phase lag of the temperature gradient ($\tau_T$), the phase lag of the heat flux is equivalent to the lagging time in the TM model and the correlating length is equivalent to the length parameter in the TM model. The resulting NL-wave propagates faster than the CV-wave, with a higher temperature in the much broader heat affected zone. The exceeding amount increases with the value of $L$, which is the ratio between $\lambda_q$ (the correlating length) to $\sqrt{(\alpha\tau_q)}$ (the diffusion length over the period of the relaxation time). The higher temperature and the faster wave speed of the NL-wave will put the dielectrics at a higher risk of thermal damage, which requires special attention in MEMS/NEMS design. The effect $\tau_T$ effectively destroys the sharp wavefront of the NL-wave, similar to its effect on the CV-wave. The nonlocal behavior in thermal lagging further raises the temperatures above those coming from the lagging behavior (from $\tau_T$ and $\tau_q$) alone.

Experimental evidences are underway to support the thermomass model/nonlocal behavior proposed herewith. Based on the ultrafast instrumentations that involve excitations of thin films by femtosecond lasers [20], the primary emphasis has been placed on the additional thermal disturbances caused by the reflection of the TM/NL-wave from the film surfaces. With one more wave model now added into the regime of microscale heat transfer, the term of "non-Fourier" behavior may need further refinement. So far we have the CV-wave resulting from the effect of $\tau_q$, the T-wave resulting from the $\tau_q^2$-effect [10], and now the NL-wave resulting from the nonlocal behavior in thermal lagging. With the tangling effects between rapid thermalization and thermal relaxation, the T-wave can be slower or faster than the NL-wave depending on the ratio of $\tau_T$ to $\tau_q$. Addition of the NL-wave will add another characteristic time in the time scale describing the wave-diffusion duality in heat transport [21].

## References

[1] C. Momma, B.N. Chichkov, S. Nolte, F.V. Alvensleben, A. Tunnermann, H. Welling, B. Wellegehausen, Short-pulse laser ablation of solid targets. Optics Communications 129 (1996) 134–142.
[2] C. Momma, S. Nolte, B.N. Chichkov, F.V. Alvensleben, A. Tunnermann, Precise laser ablation with ultrashort pulses. Applied Surface Science 109 (1997) 15–19.
[3] S. Preuss, A. Demchuk, M. Stuke, Sub-picosecond UV laser ablation of metals. Applied Physics A 61 (1995) 33–37.
[4] M.D. Shirk, P.A. Molian, A review of ultrashort pulsed laser ablation of materials. Journal of Laser Applications 10 (1998) 18–28.
[5] B.C. Stuart, M.D. Feit, S. Herman, A.M. Rubenchik, B.W. Shore, M.D. Perry, Optical ablation by high-power short-pulse lasers. Journal of the Optical Society of America B 13 (1996) 459–468.
[6] J.M. Hopkins, W. Sibbett, Ultrashort-pulse lasers: big payoffs in a flash. Scientific American 283 (2000) 72–79.
[7] D.Y. Tzou, J.K. Chen, J.E. Beraun, Recent development of ultrafast thermoelasticity. Journal of Thermal Stresses 28 (2005) 563–594.
[8] T.Q. Qiu, C.L. Tien, Short-pulse laser heating on metals. International Journal of Heat and Mass Transfer 35 (1992) 719–726.
[9] T.Q. Qiu, C.L. Tien, Heat transfer mechanisms during short-pulse laser heating of metals. ASME Journal of Heat Transfer 115 (1993) 835–841.
[10] D.Y. Tzou, Macro- to Microscale Heat Transfer: The Lagging Behavior. Taylor & Francis, Washington, D.C., USA, 1997.
[11] C. Cattaneo, A form of heat conduction equation which eliminates the paradox of instantaneous propagation. Compte Rendus 247 (1958) 431–433.
[12] P. Vernotte, Les paradoxes de la théorie continue de l'équation de la chaleur. Compte Rendus 246 (1958) 3154–3155.
[13] R.A. Guyer, J.A. Krumhansl, Solution of the linearized Boltzmann equation. Physical Review 148 (1966) 766–778.
[14] M.E. Gurtin, A.G. Pipkin, A general theory of heat conduction with finite wave speed. Archive for Rational Mechanics and Analysis 31 (1968) 113–126.
[15] D.Y. Tzou, W. Dai, Thermal lagging in multi-carrier systems. International Journal of Heat and Mass Transfer 52 (2009) 1206–1213.
[16] D.Y. Tzou, Lagging behavior in biological systems, in: 2nd ASME International Conference on Micro/Nanoscale Heat and Mass Transfer, December 18–21, 2009, Shanghai, China.
[17] B.Y. Cao, Z.Y. Guo, Equation of motion of a phonon gas and non-Fourier heat conduction. Journal of Applied Physics 102 (2007) 053503.
[18] Z.Y. Guo, Q.W. Hou, Thermal wave based on the thermomass model, ASME Journal of Heat Transfer, in press.
[19] D.Y. Tzou, Computational techniques in microscale heat transfer. in: W.J. Minkowycz, E.M. Sparrow, J.Y. Murphy (Eds.), Handbook of Numerical Heat Transfer, second ed. Wiley, New York, 2006, pp. 623–657 (Chapter 20).
[20] S.D. Brorson, J.G. Fujimoto, E.P. Ippen, Femtosecond electron heat-transport dynamics in thin gold film. Physical Review Letters 59 (1987) 1962–1965.
[21] D.Y. Tzou, Thermal lagging: duality of diffusion and wave in ultrafast transient, keynote lecture. in: The 7th International Symposium on Heat Transfer, October 26–29, 2008, Beijing, China.